

RM-532J

THE EFFECT OF CONE ANGLE
ON PENETRATION RESISTANCE

January 1972

R E S E A R C H D E P A R T M E N T

Reproduced by
**NATIONAL TECHNICAL
INFORMATION SERVICE**
Springfield, Va 22151

GRUMMAN AEROSPACE CORPORATION
BETHPAGE NEW YORK

Security Classification

DOCUMENT CONTROL DATA - R & D

(Security classification of title, body of abstract and indexing annotation must be entered when the overall report is classified)

1. ORIGINATING ACTIVITY (Corporate author)		2a. REPORT SECURITY CLASSIFICATION Unclassified
Grumman Aerospace Corporation		2b. GROUP n/a
3. REPORT TITLE The Effect of Cone Angle on Penetration Resistance		
4. DESCRIPTIVE NOTES (Type of report and inclusive dates) Research Memorandum		
5. AUTHOR(S) (First name, middle initial, last name) Edward A. Nowatzki Leslie L. Karafiath		
6. REPORT DATE January 1972	7a. TOTAL NO. OF PAGES 27	7b. NO. OF REFS 15
8a. CONTRACT OR GRANT NO. none	9a. ORIGINATOR'S REPORT NUMBER(S) RM-532J	
b. PROJECT NO. c. d.	9b. OTHER REPORT NO(S) (Any other numbers that may be assigned this report) none	
10. DISTRIBUTION STATEMENT Approved for public release; distribution unlimited		
11. SUPPLEMENTARY NOTES none	12. SPONSORING MILITARY ACTIVITY n/a	
13. ABSTRACT Cone penetrometers offer a relatively quick and simple method of measuring <u>in situ</u> soil strength properties. The cone penetrometer developed by the U.S. Army Corps of Engineers Waterways Experiment Station (WES) is widely used in off-road mobility research and in the evaluation of flotation capability of aircraft landing gear on unprepared runways. Cone penetrometers were also used to determine <u>in situ</u> strength of the lunar soil. Despite the wide use of cone penetrometers, only approximate theories are available to evaluate the shear strength parameters from the measured cone penetration resistance or "cone index." In this memorandum a theoretical analysis, based on the numerical solution of the differential equations of plasticity, is presented that takes into account correctly both the axial symmetry and the friction at the surface of the cone. The resistance of penetrometers having various various cone apex angles is determined by this method for a range of soil properties. The computed cone indices are compared with those measured in the laboratory. Conclusions are drawn regarding the efficacy of the cone penetrometer as a measure of soil strength and recommendations are made to help resolve the ambiguities inherent in the cone index measurement.		

DD FORM 1 NOV 65 1473

Security Classification

Security Classification

14 KEY WORDS	LINK A		LINK B		LINK C	
	ROLE	WT	ROLE	WT	ROLE	WT
Elasticity Theory Coulomb Failure Criterion Slip Line Field Geometry Soil Compressibility Penetrometer Data Soil Bearing Capacity						

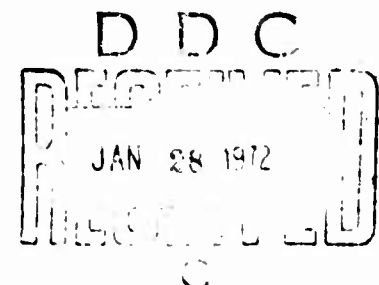
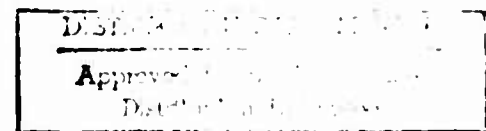
THE EFFECT OF CONE ANGLE ON PENETRATION RESISTANCE[†]

by

E. A. Nowatzki and L. L. Karafiath

Materials and Structural Mechanics Section

January 1972



[†]Accepted paper for Annual Meeting of Highway Research Board, Washington, D.C., January 17-21, 1972.

Approved by: *Charles E. Mack, Jr.*
Charles E. Mack, Jr.
Director of Research

The Effect of Cone Angle on Penetration Resistance

Edward A. Nowatzki and Leslie L. Karafiath

Research Department
Grumman Aerospace Corporation
Bethpage, New York 11714

ABSTRACT

Static and dynamic cone penetration tests are widely used in the field and laboratory to obtain comparative measures of soil strength. Theoretically rigorous methods of analysis of the penetration process are nonexistent; approximate methods have only limited applicability.

A theoretically correct three dimensional analysis of cone penetration using plasticity theory and the Coulomb failure criterion is presented. The differential equations of plastic equilibrium are solved numerically for an ideal uniform dry sand to show the variation of slip line field geometry with changes in the apex angle of the cone. The results indicate that with increasing apex angle, less soil volume is affected. The results of a series of laboratory tests using variously angled cones on Jones Beach sand are plotted to show how the value of cone index increases with increasing apex angle. Cone index is defined as the ratio of the soil resistance to the base area of the cone. The differential equations of plastic equilibrium are again solved numerically

for soil and boundary conditions that correspond to those of the experiments. These results support the validity of the theory in dense sands. The experimental results also demonstrate that soil compressibility affects the cone index to the extent that it no longer serves as a measure of frictional strength. For loose soils, differences in cone angles have little effect on cone index, all other conditions being equal. To identify this condition it is recommended that two cones be used in penetrometer tests, one having an obtuse apex angle, the other an acute apex angle.

The theoretical and experimental results are correlated to show how the theory may be used for any soil to predict the angle of internal friction.

1. Introduction

The merits of using penetrometer data for determining soil properties have been discussed extensively [Fletcher, G. (1965), Meyerhof, G. G. (1956), Schultze, E. and Knausenberger, H. (1957)]. In many of these reports empirical expressions are derived purporting to relate penetration test parameters to soil properties, for example, blow count data of the Standard Penetration Test (SPT) to the relative density of the soil being penetrated. Although most of the effort has been directed toward dynamic tests such as the SPT, some consideration has also been given to relating soil parameters to static cone penetration characteristics (WES, 1964).

At any rate, very little attention has been paid to a theoretical analysis of the interaction between a cone penetrometer and the failing soil during the penetration process, although there exists in the literature a well established basis for such a study. The following paragraph presents a brief review of the pertinent contributions in the area of plasticity analysis of soils' problems.

The theory of static equilibrium has been combined with the Coulomb failure criterion and applied to studies of soil bearing capacity. Prandtl (1920) solved the resulting differential equation of plastic equilibrium for a strip footing on weightless soil (plane strain condition). Cox, Eason, and Hopkins (1961) developed a general theory of axially-symmetric plastic deformations in ideal soils and applied it to the problem of the penetration of a smooth, rigid, flat-ended circular cylinder into a semi-infinite mass of weightless soil. Drucker and Prager (1952) and more recently Spencer (1962) extended the theory for the plane strain case to include body forces such as soil weight and cohesion; while Cox (1962) and more recently Larkin (1968) did the same for the axially-symmetric case. In cases where the characteristic relations for the governing differential equations cannot be integrated explicitly, numerical methods are used. Sokolovskii (1965) presented the most widely used procedure of numerical integration, a finite difference approximation based on the method of characteristics.

Studies relating specifically to cone indentation problems are less numerous. Sneddon (1965) derived a solution to the cone indentation problem within the framework of the classical theory of elasticity. Meyerhof (1961) and Berezantzev (1967) offered approximate solutions of the axially-symmetric problem. The former applied the solution to a study of the effect of surface roughness on cone penetration; the latter investigated the use of penetrometer data to determine friction angle.

2. Objective

An analysis is presented of the penetration of a perfectly rigid cone into an ideal granular soil whose strength properties are defined by the Coulomb failure criterion. Plastic stress states are considered to be symmetric with the central axis of a right circular cone. A purely frictional soil is assumed so that local pore pressure buildup may be neglected. This assures that failure occurs in shear zones rather than along a single failure surface. In the model used in the analysis the limit load, obtained from a solution which satisfies the basic differential equations of plasticity and the boundary stress condition, is considered a lower bound (Drucker and Prager, 1952).

3. Scope

This study is arranged in the following order. In Section 4 the variables are identified and defined. Section 5 contains the governing equations of plastic equilibrium for the axially-symmetric case. In Section 6 the limitations of the present investigation are discussed. The major results obtained from the theory within those limitations are presented and discussed with reference to experimental data. Conclusions are drawn at this point in the analysis. Finally, in Section 7 the results of this study are summarized and remarks made concerning them and their relation to future research in this area.

4. Notation

The quantities defining the geometry of the problem are given in Fig. 1.

A_o = area of cone base

c = cohesion

G = slip line geometry similitude factor

CI = cone index, defined in psi as the penetration resistance/ A_o where, in this study, the resistance at 6-in. penetration is used as a reference

R_o = radius of cone base

w = surcharge

r, z = coordinates

z_0 = depth to which base of cone has penetrated
 α = apex angle of cone or cone angle
 β = complement to apex semi-angle
 γ = unit weight of soil
 δ = friction angle between cone and soil
 θ = angle between r axis and major principal stress
 ϕ = angle of internal friction of soil
 ψ = $c \cot \phi$
 μ = $\pi/4 - \phi/2$
 σ = $(\sigma_1 + \sigma_3)/2 + \psi$ (in general)

5. Formulation

The following set of differential equations represents the theoretically rigorous formulation to the problem of determining axially-symmetric plastic stress states and slip line fields.

$$\begin{aligned}
 d\sigma \pm 2\sigma \tan \phi d\theta - \frac{\gamma}{\cos \phi} (\sin(\pm \phi) dr + \cos(\pm \phi) dz) + \\
 \frac{\sigma}{r} (\sin \phi dr \pm \tan \phi (1 - \sin \phi) dz) = 0 \\
 dz = dr \tan(\theta \pm \mu) . \quad (1)
 \end{aligned}$$

This set of equations is obtained by combining the equations of equilibrium derived from plasticity theory with the Coulomb failure criterion. The circumferential stress is assumed to be the intermediate principal stress and to be equal to the minor principal

stress (σ_3). The r -axis of the coordinate system is parallel to the ground surface and the positive z -axis is perpendicular to it into the soil mass (see Fig. 1). The upper sign refers to the family of slip lines corresponding to the first characteristics of the differential equations (i-lines), and the lower sign to the second (j-lines).

No closed form solution to these equations exists. Several numerical solutions have been presented; however, these are restricted to the axially-symmetric surface loading of the semi-infinite half space. The equations below are the numerical form of Eqs. (1) used to study the effect of soil properties and cone parameters on the penetration characteristics of a right circular cone penetrating soil. To keep the problem perfectly general, soil body forces have been included in the formulation. For a given set of loading conditions (w) over the horizontal soil surface, the values of $r_{i,j}$, $z_{i,j}$, $\sigma_{i,j}$, and $\theta_{i,j}$ are computed for an adjacent nodal point (slip line intersection point; refer to Fig. 1) by use of the set of recurrence relationships:

$$r_{i,j} = (z_{i-1,j} - z_{i,j-1} + \epsilon_1 r_{i,j-1} - \epsilon_2 r_{i-1,j}) / (\epsilon_1 - \epsilon_2) \quad (2)$$

$$z_{i,j} = z_{i-1,j} + (r_{i,j} - r_{i-1,j}) \epsilon_2 \quad (3)$$

where $r_{i,j}$ and $z_{i,j}$ are the coordinates of the adjacent nodal point, and $\epsilon_1 = \tan(\theta_{i,j-1} + \mu)$, $\epsilon_2 = \tan(\theta_{i-1,j} - \mu)$. With these values of $r_{i,j}$ and $z_{i,j}$ the computation is continued for

$$\sigma_{i,j} = \left[2\sigma_{i-1,j} \sigma_{i,j-1} (1 + \tan \varphi(\theta_{i,j-1} - \theta_{i-1,j})) + \sigma_{i-1,j}^D \right. \\ \left. + \sigma_{i,j-1}^C - \sigma_{i,j-1} \sigma_{i-1,j} (B/r_{i,j-1} + A/r_{i-1,j}) \right] / (\sigma_{i,j-1} + \sigma_{i-1,j}) \quad (4)$$

$$\theta_{i,j} = \left[\sigma_{i,j-1} - \sigma_{i-1,j} + 2 \tan \varphi(\sigma_{i,j-1} \theta_{i,j-1} + \sigma_{i-1,j} \theta_{i-1,j}) \right. \\ \left. + D - C + \sigma_{i-1,j} A/r_{i-1,j} - \sigma_{i,j-1} B/r_{i,j-1} \right] / 2 \tan \varphi(\sigma_{i,j-1} + \sigma_{i-1,j}) \quad (5)$$

where

$$A = \sin \varphi(r_{i,j} - r_{i-1,j}) - \tan \varphi(1 - \sin \varphi)(z_{i,j} - z_{i-1,j}) \quad (6)$$

$$B = \sin \varphi(r_{i,j} - r_{i,j-1}) + \tan \varphi(1 - \sin \varphi)(z_{i,j} - z_{i,j-1}) \quad (7)$$

$$C = \gamma(z_{i,j} - z_{i-1,j} - \tan \varphi(r_{i,j} - r_{i-1,j})) \quad (8)$$

$$D = \gamma(z_{i,j} - z_{i,j-1} + \tan \varphi(r_{i,j} - r_{i,j-1})) \quad (9)$$

To apply these recurrence relationships to the problem of cone indentation, the geometric boundary conditions as well as the stress boundary conditions had to be formulated appropriately and included in the computer program. The geometric boundary conditions are simply mathematical descriptions of the cone geometry

and its position at depth in terms of r , z , α , and R_o . The stress boundary conditions and the method of computation are essentially the same as those described by the authors elsewhere for two dimensional conditions (Karafiath and Nowatzki, 1970).

Briefly, the stress boundary condition on the horizontal plane through the base of the cone is given by the surcharge (w) and the overburden soil pressure (see Fig. 1). Overburden shear is disregarded. The slip-line field in the passive zones is computed by Eqs. (1) starting with these boundary values and an assumed value for the horizontal extent of the passive zone. In the radial shear zone, the same equations are used, but special consideration is given to the central point where the j -lines converge (point Q in Fig. 1). This point is a degenerated slip line, where θ changes from the value at the passive boundary to that specified at the active zone boundary. The total change in θ is divided by the number of slip lines converging at this point to obtain an equal $\Delta\theta$ increment between two adjacent slip lines. The σ values for each increment are computed from the equation $\sigma = \sigma_o e^{2(\theta - \theta_o)\tan \phi}$, which is the solution to Eqs. (1) if both dr and dz vanish. Allowance must be made for the angle β as well as δ in assigning transition values of θ and σ between the active and passive zones. With these values of θ and σ for each slip line at this point, the coordinates as well as the σ

and θ values for all other points in the radial shear zone can be computed by Eqs. (1). In the active zone the same equations are used, except for the points at the loaded surface of the cone itself, where $\theta_{i,j}$ is assigned and $z_{i,j} = z_o + (R_o - r_{i,j}) \tan \alpha$.

Here:

$$r_{i,j} = \frac{r_{i-1,j} \tan((\theta_{i,j} + \theta_{i-1,j})/2 - \mu) - z_{i-1,j} + R_o \tan \alpha + z_o}{\tan((\theta_{i,j} + \theta_{i-1,j})/2 - \mu) + \tan \alpha} \quad (10)$$

$$\sigma_{i,j} = \sigma_{i-1,j} + \sigma_{i-1,j} (\theta_{i,j} - \theta_{i-1,j}) \tan \phi + C - \frac{\sigma_{i-1,j}^A}{r_{i-1,j}}. \quad (11)$$

The numerical computation is performed and adjustments made, if necessary, to the value assumed for the horizontal extent of the passive zone until the slip line field "closes" on the axis of symmetry at the apex of the cone.

6. Results and Conclusions

a. Theoretical Results - Slip Line Field Geometries

The numerical computation of the slip line field geometries and associated stresses by the recurrence relationships [Eqs. (2) through (5)] was performed on an Adage Inc. time-sharing computer system. This system is based on Digital Equipment Corporation PDP-10 processors. To show specifically the effect of cone angle on the slip line field geometry, the governing differential equations

were solved for a set of ideal soil conditions that describe a homogeneous, dry, and purely frictional sand. These conditions are $c = 0$, $\phi = 37^\circ$, $\gamma = 100$ pcf, $w = 1$ psf, and $\delta = 20^\circ$. The numerical results were plotted automatically and electronically on the display tube of a Computer Displays Inc. Advanced Remote Display System. The slip line fields for $R_o = 0.034$ ft (radius of the WES cone) and $\alpha = 15.5^\circ, 30^\circ, 60^\circ, 90^\circ, 120^\circ$, and 150° have been reproduced and are shown in Figs. 2. Since the problem is axially-symmetric, only half the total field has been shown; the dashed line indicates the central axis of the cone. The geometric scale may be obtained for each figure from the knowledge that the base radius of the cone is 0.4 in. The scale in Fig. 2a is four times that in Fig. 2b.

For given soil strength parameters c and ϕ the slip line fields representing the solution of the differential equations are geometrically similar only if the ratio $G = \gamma\ell/(c+w \tan \phi)$ is the same (Cox, 1962), where ℓ is a characteristic length usually taken equal to R_o . Although the slip line geometry similitude factor G , as defined by Cox for the case of bearing capacity, is the same (4.512) in all of the cases represented in Figs. 2, it is obvious that the slip line geometries differ, an indication that the G -equality is a necessary but not sufficient condition for slip line field similitude. In addition to G , there must

also be equality in δ and a similitude in the geometric condition at both the free and loaded boundaries to obtain complete geometric similitude of the slip line field.

The salient feature of Figs. 2 is that they distinctly show a contraction of the radial shear zone with decrease in cone angle. In Fig. 2b the contraction is so pronounced that the individual i- and j-lines are hardly discernible with the scale used. The active, passive, and radial shear zones all have curvilinear boundaries due to the three dimensional nature of the problem, an indication that the geometries obtained from the solution of the theoretically-correct differential equations differ from those obtained by using the Prandtl solution for weightless soil and the log-spiral approximation in the radial zone.

Also indicated by Figs. 2 is the fact that, with decreasing cone angle, the affected volume of soil increases. For the soil and cones used in Figs. 2, the volume of the body of revolution formed by the slip line field for $\alpha = 30^\circ$ is about ten times greater than that for $\alpha = 150^\circ$. For compressible soils, the size of the affected mass directly influences the load-penetration relationship. The material must be compressed to a state in which friction is fully mobilized before shear failure along slip lines can take place. The load necessary to accomplish this compression is usually less than the load needed to fail the soil in shear. It

follows that the larger the volume of the slip line field, the more the soil mass must be compressed to mobilize the friction fully. Therefore, cone indices obtained with cone shapes that result in large-volume slip line fields are likely to be less representative of the Coulombic strength than of the compressibility of the material.

b. Experimental Results

A series of penetration tests were conducted on Jones Beach sand using aluminum cones. The friction angle between the aluminum surface of the cone and the sand was assumed to be uniform and equal to 15 degrees on the basis of experiments performed by Mohr and Karafiath (1967). The purpose of the tests was to determine the effect of cone angle (α) on the value of the cone index (CI). The base area of cones having apex angles of 150, 90, and 30 degrees was 0.5-in.^2 . The 30-degree cone corresponds to the WES cone. Also used was a cone having a base area of 1.04-in.^2 and an apex angle of 15.5 degrees. This cone corresponds to that used until 1956 by the North Dakota State Highway Department for flexible pavement design. The physical properties of Jones Beach sand are listed in Table 1. Uniform soil beds were prepared to a narrow range of desired densities in a facility specially designed for this purpose.

To conduct the tests, the cones were attached interchangeably to a 12-in. rod and the entire assembly mounted on the loading frame of an Instron testing instrument Model TM-M (Fig. 3). The rate of penetration was set at 10 cm/min. Load-penetration curves were obtained automatically on a synchronized strip-chart recorder. Values of CI as defined for this study were determined directly from the load-penetration curves. The results of the penetration test series are given in Figs. 4 and 5.

Figure 4 shows the variation of cone index with change in cone angle for Jones Beach sand at various relative densities. It is clear from the figure that when the material is loose ($88 \text{ pcf} \leq \gamma < 94 \text{ pcf}$) the cone angle has very little effect on the cone index (all values of CI are less than approximately 9 regardless of the size of the cone angle). On the other hand, for dense materials ($100 < \gamma \leq 105$) CI varies from approximately 19 for the 15.5 degree cone to between 44 and 60 for the 150 degree cone. These results seem to verify the previously discussed effect of compressibility on the value of cone index. Apparently the frictional strength of the loose material cannot be fully mobilized until the material is sufficiently compressed to allow for complete shear failure. Calculations made on the basis of volume change properties of the Jones Beach sand indicated that the average percent volume change of the soil mass within the slip

line field was virtually independent of the apex angle of cones having the same base area. Consequently, the displacement necessary to mobilize the full friction is roughly proportional to the volume of the slip line field. These results suggest that, in order to use the cone index as a valid measure of the frictional strength of a soil, two cones should be used, both having the same base area but one having an obtuse apex angle, the other an acute apex angle. If the values of CI obtained from these two cones are similar, then the penetration resistance is governed by the compressibility of the soil. If on the other hand, the two values are markedly different, then a relationship may properly be sought between CI and the strength parameters of the material.

Of course, the problem is not entirely that simple. In addition to the compressibility effect at lower relative densities, there is the effect of the variation of ϕ with γ . Figure 5 shows for each of the cones investigated the change in cone index with variation of unit weight. It is impossible from such a plot to distinguish which of the two effects has the greater influence. However, it seems reasonable to assume that, in the range of unit weights over which the material may be considered relatively dense, the compressional effect is negligible.

c. Comparison between Experimental and Theoretical Results

In Fig. 6 the experimentally obtained values of CI are compared over a wide range of unit weights with the values determined

theoretically by the solution of the differential equations of plastic equilibrium. For clarity, only the results for the 150 degree cone are presented. The theoretical curves suggest that for ϕ constant there is little change in CI with variation in γ . The theoretical curves also show that for a given unit weight the value of CI is very sensitive to changes in ϕ . The experimental curve, which shows a pronounced decrease of CI with decrease in γ , not only reflects the change in ϕ with unit weight and stress level (refer to Table 1), but also includes the effect of soil compressibility discussed above. Unfortunately, the experimental curve itself does not distinguish between these effects; however, for reasons cited above it seems that the compressibility has the least influence on tests performed with dense material. For example, from Fig. 6 a cone index of 43 for Jones Beach sand at 103 pcf indicates a ϕ -angle of approximately 38-39 degrees. For the stress level involved, this value of ϕ determined from cone penetrometer data agrees quite well with the values obtained from triaxial tests listed in Table 1.

Therefore, although the theory of plastic equilibrium has not been modified in this study to include in the computation of CI the effects of a curvilinear Mohr envelope (Berezantzev and Kovalev, 1968; Szymanski, 1958), or the contribution of soil compressibility, we believe that curves such as those presented in Fig. 6 can be used to estimate an average value of ϕ from cone penetrometer data.

7. Summary and Discussion

The major results of the present investigation are summarized as follows:

a. For the axially-symmetric case, the slip line field geometry derived from the theory of plastic equilibrium for a dry, uniform sand being penetrated by a cone differs markedly from that obtained by the Prandtl solution for weightless soil and the log-spiral approximation.

b. For materials at high relative densities, the cone index varies significantly with the size of the penetrometer apex angle, all other conditions being equal. This is not observed for loose materials. Soil compressibility, the variation of ϕ with γ , and the curvilinear nature of the Mohr failure envelope can account for this difference in performance.

c. Solutions derived from the theory of plastic equilibrium agree well with experimentally obtained cone penetrometer data and can be used, under certain conditions, to estimate the strength parameter ϕ for a dense dry sand. In all penetrometer investigations the use of two cones is recommended to avoid misinterpretation of the cone index. One cone should have an obtuse apex angle, the other an acute angle.

Further investigations are needed to enhance the theory presented in this study. For example, it would be very desirable to incorporate into the computer program the curvilinearity of the Mohr envelope and the dependence of ϕ on unit weight. Similarly, the effect of compressibility on the penetration resistance of a material should be expressed quantitatively, and criteria for the mobilization of friction in the slip line field established.

8. References

Berezantzev, V. G. (1967), "Certain Results of Investigation on the Shear Strength of Sands," Proceedings of the Geotechnical Conference, Oslo, Vol. 1, pp. 167-169.

Berezantzev, V. G. and Kovalev, I. V. (1968), "Consideration of the Curvilinearity of the Shear Graph when Conducting Tests on Model Foundations," translated from Osnovaniya, Fundamenty i Mekhanika Gruntov, No. 1, pp. 1-4.

Cox, A. D. (1962), "Axially-Symmetric Plastic Deformation in Soils - II Indentation of Ponderable Soils," International Journal of Mechanical Sciences, Vol. 4, pp. 371-380.

Cox, A. D., Eason, G., and Hopkins, H. G. (1961), "Axially-Symmetric Plastic Deformation in Soils," Transactions, Royal Society of London, Vol. 254A, pp. 1-45.

Drucker, D. C. and Prager, W. (1952), "Soil Mechanics and Plastic Analysis or Limit Design," Quarterly of Applied Mathematics, Vol. 10, No. 2, pp. 157-165.

Fletcher, G. (1965), "The Standard Penetration Test: Its Uses and Abuses," Proceedings ASCE, SM & FD, Vol. 91, SM 4, pp. 67-76.

Karafiath, L. L. and Nowatzki, E. A. (1970), "Stability of Slopes Loaded over a Finite Area," Highway Research Board Record No. 323, November 1970.

Larkin, L. A. (1968), "Theoretical Bearing Capacity of Very Shallow Footings," Proceedings ASCE, SM & FD, Vol. 94, SM 6, pp. 1347-1357.

Meyerhof, G. G. (1956), "Penetration Tests and Bearing Capacity of Cohesionless Soils," Proceedings ASCE, SM & FD, Vol. 82, No. SM 1, pp. 1-19.

Meyerhof, G. G. (1961), "The Ultimate Bearing Capacity of Wedge-Shaped Foundations," Proceedings of the Fifth International Conference on Soil Mechanics and Foundation Engineering, Paris, Vol. 2, pp. 105-109.

Mohr, G. and Karafiath, L. L. (1967), Determination of the Coefficient of Friction between Metals and Nonmetals in Ultrahigh Vacuum, Grumman Research Department Report RE-311, December 1967.

Prandtl, L. (1920), "Über die Harte Plastischer Körper," Göttingen Nachr, Math Phys. Kl., p. 74.

Schultz, E. and Knausenberger, H. (1957), "Experiences with Penetrometers," Proceedings, Fourth International Conference on Soil Mechanics and Foundation Engineering, Vol. 1, pp. 249-255.

Sneddon, I. N. (1965), "The Relation between Load and Penetration in the Axisymmetric Boussinesq Problem for a Punch of Arbitrary Profile," International Journal of Engineering Science, Vol. 3, pp. 47-57.

Sokolovskii, V. V. (1965), Statics of Granular Media, Pergamon Press.

Spencer, A. J. M. (1962), "Perturbation Methods in Plasticity - III Plane Strain of Ideal Soils and Plastic Solids with Body Forces," Journal of the Mechanics and Physics of Solids, Vol. 10, pp. 165-177.

Szymanski, C. (1958), "Some Plane Problems of the Theory of Limiting Equilibrium of Loose and Cohesive, Non-Homogeneous Isotropic Media in the Case of a Non-Linear Limit Curve," in Non Homogeneity in Elasticity and Plasticity, ed. by W. Olszak, Pergamon Press.

W. E. S. (1964), Soil Properties in Vehicle Mobility Research; Measuring Strength-Density Relations of an Air-Dry Sand, Technical Report No. 3-652, U.S. Army Engineer Waterways Experiment Station, August 1964.

TABLE 1

ANGLE OF INTERNAL FRICTION OBTAINED FROM
TRIAXIAL TESTS ON JONES BEACH SAND

Range of γ	Range of ϕ over Normal Stress Levels of Interest
103.5 - 105.5 pcf	41° - 37°
95.5 - 97.5 pcf	38° - 30°

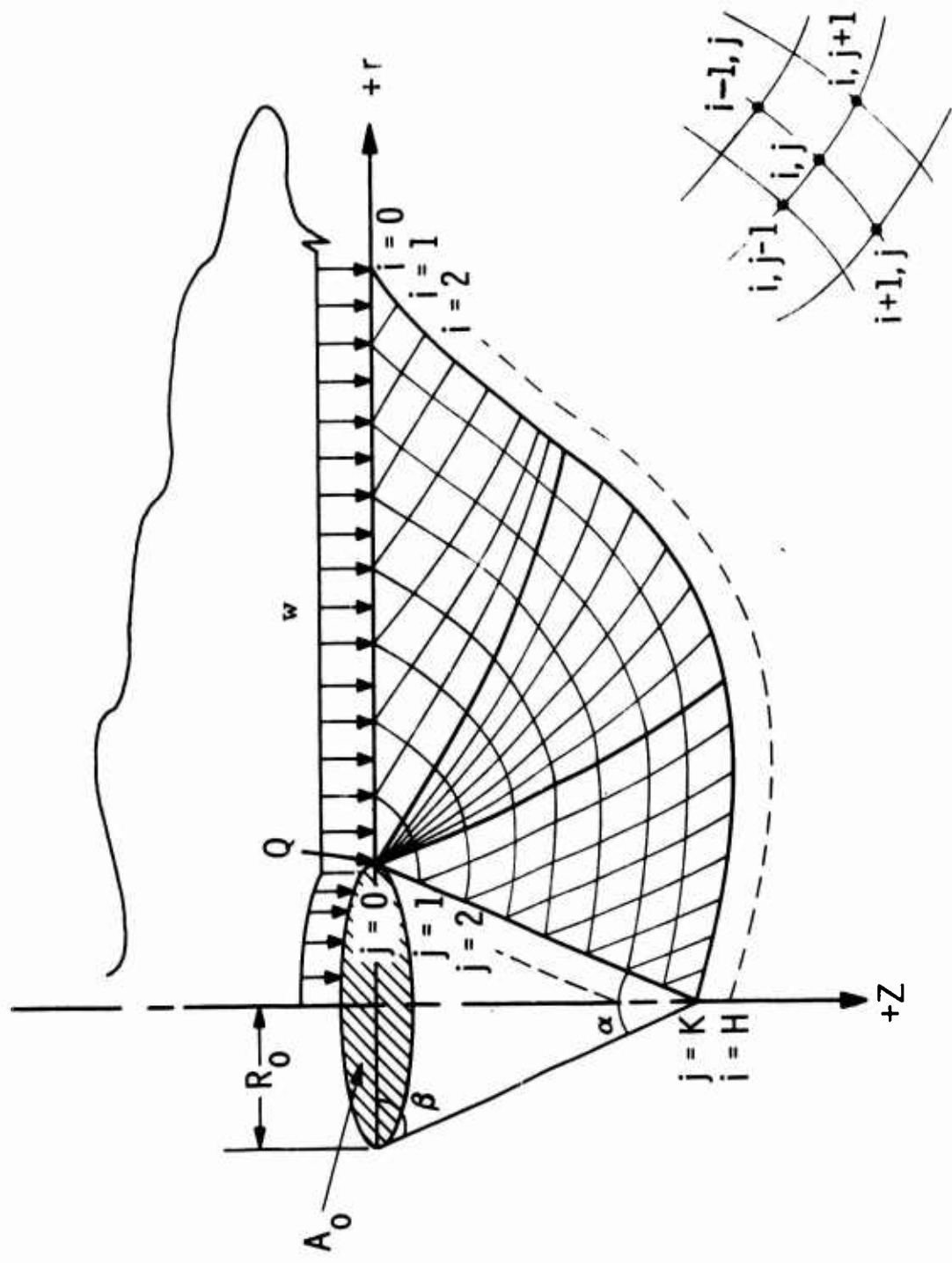


Fig. 1 Geometry for Cone Indentation Problem. Boundary conditions and slip lines are symmetric with the z -axis.

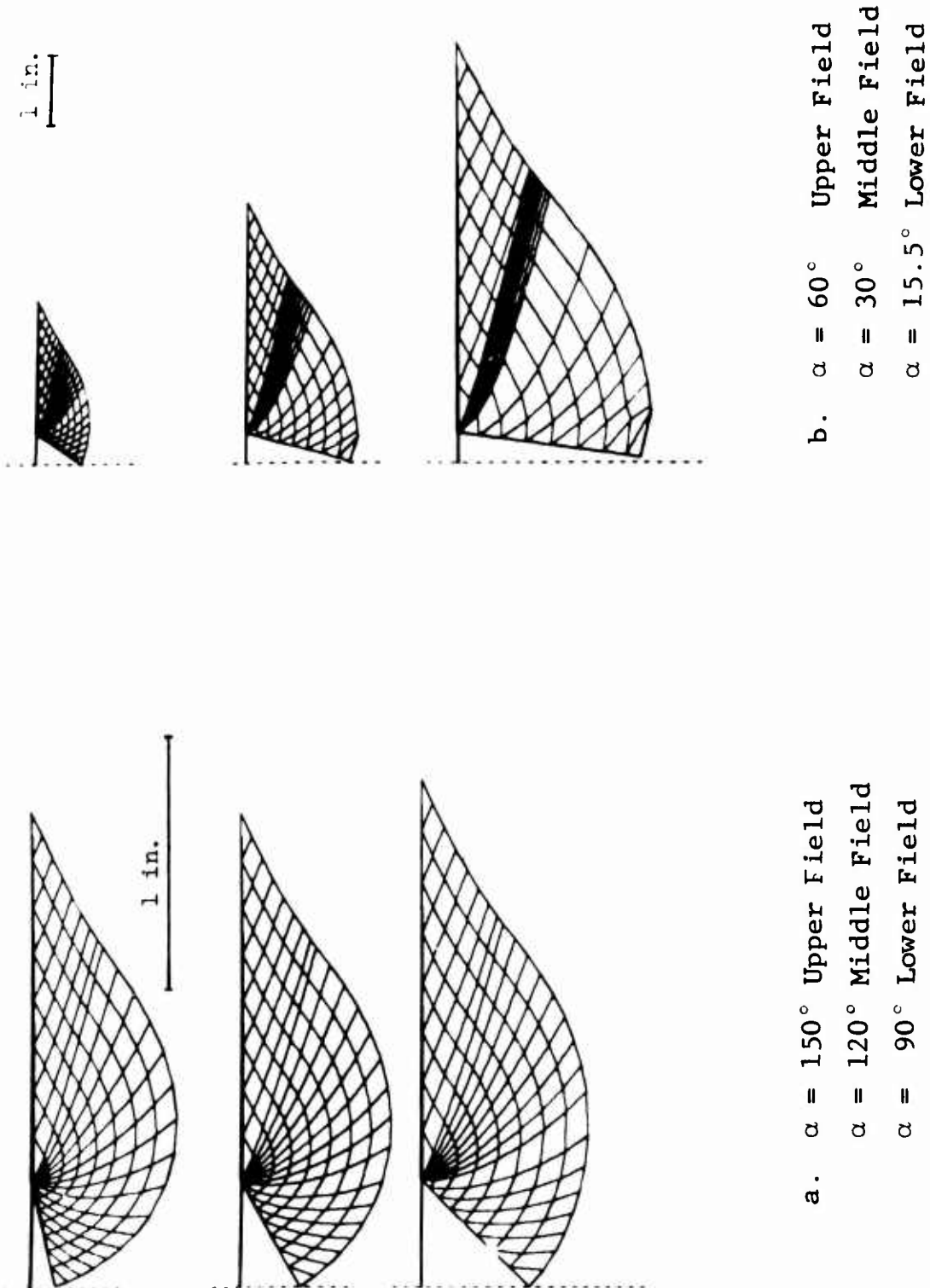


Fig. 2 Slip Line Fields for Cones Penetrating Ideal Soil

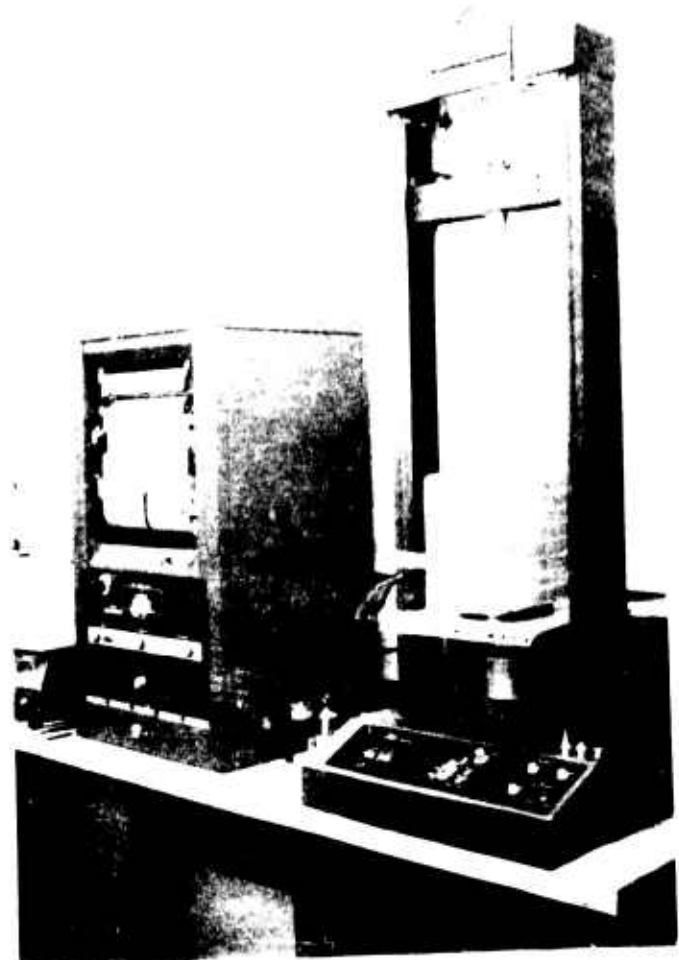


Fig. 3 Cone Penetrometer Test - Loading
and Recording Equipment

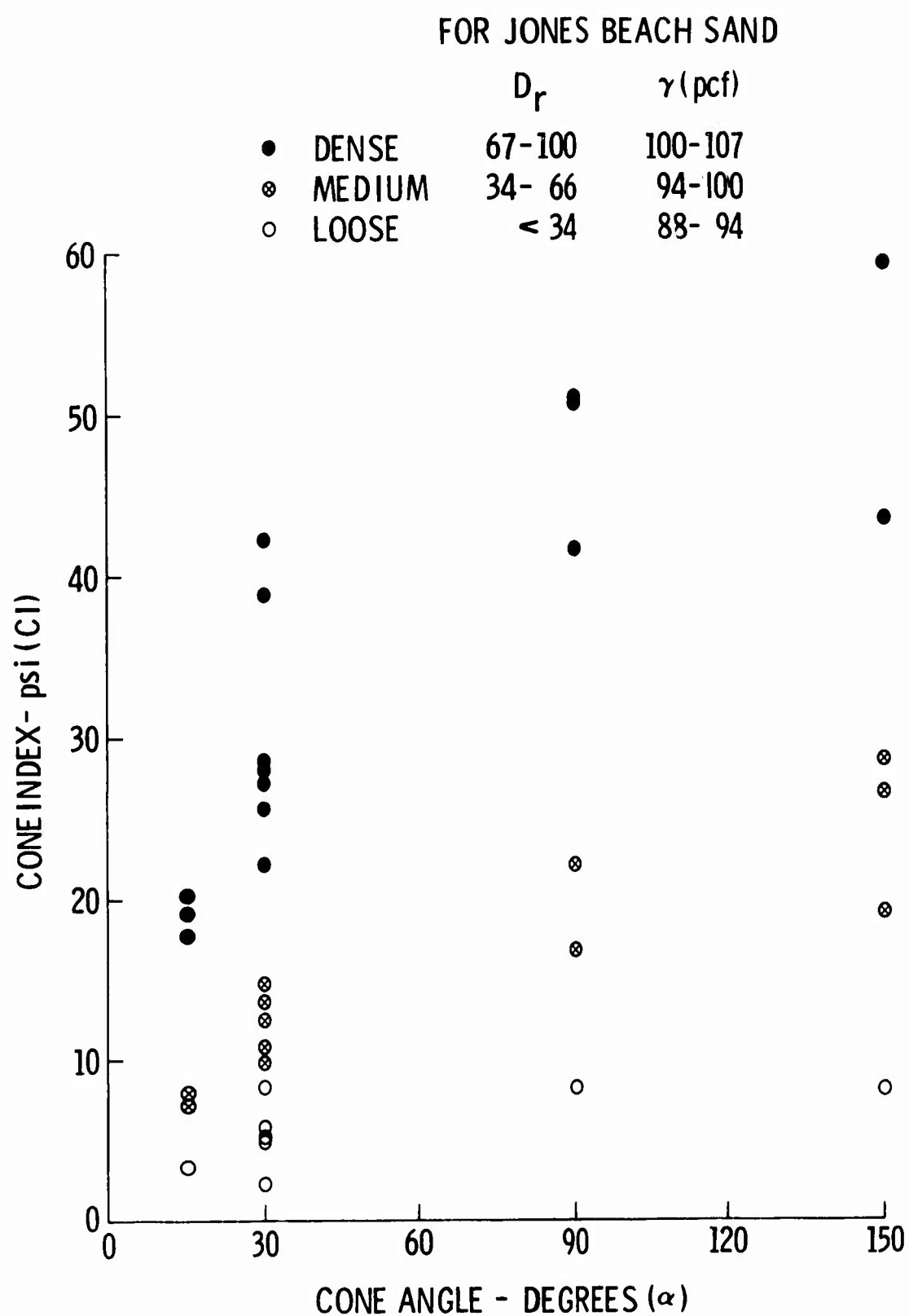


Fig. 4 Cone Index at 6-in. Penetration versus Cone Angle for Jones Beach Sand at Various Relative Densities. Experimental results.

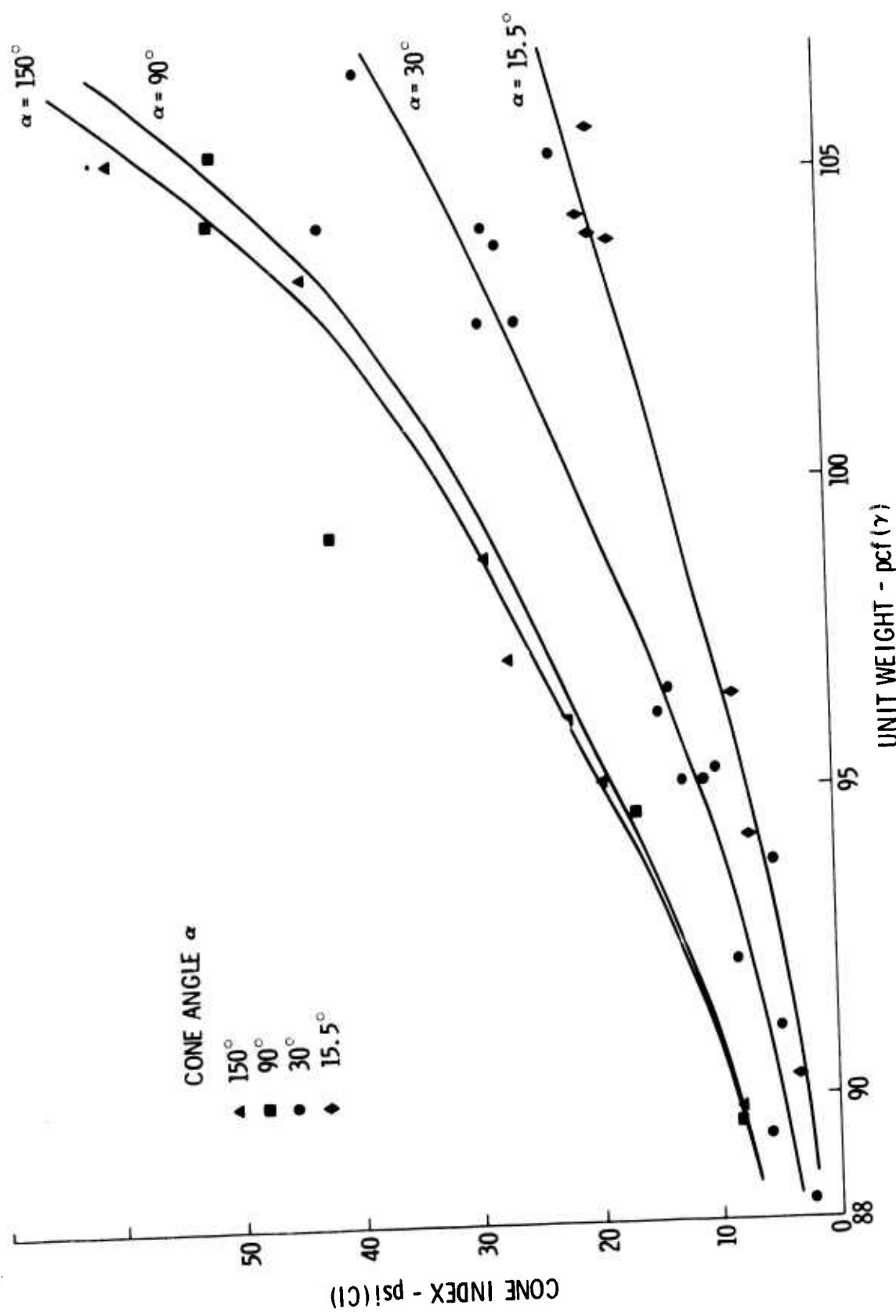


Fig. 5 Cone Index at 6-in. Penetration versus Unit Weight for Cones Having Different Apex Angles

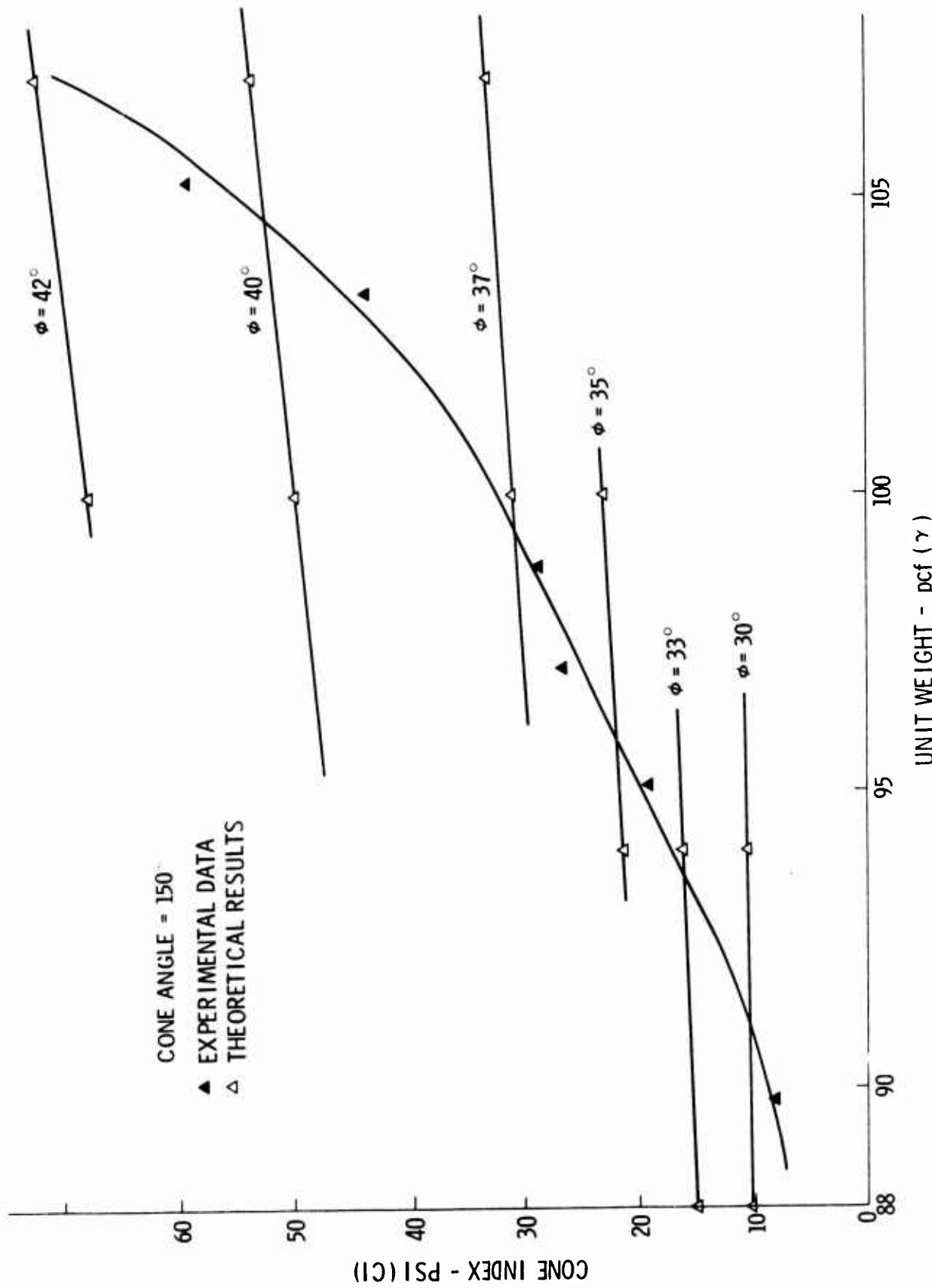


Fig. 6 Cone Index at 6-in. Penetration versus Unit weight for 150° Cone. Experimental and theoretical results.